Emerald International Journal of Numerical Methods for Heat and Fluid Flow

Mach Number Effects on Buffeting Flow on a Half Wing-body Configuration

Journal:	*International Journal of Numerical Methods for Heat and Fluid Flow*
Manuscript ID	HFF-07-2015-0283.R1
Manuscript Type:	Research Article
Keywords:	Buffet, transonic, unsteady RANS, wing-body configuration

Note: The following files were submitted by the author for peer review, but cannot be converted to PDF. You must view these files (e.g. movies) online.

figures.tar.gz

SCHOLARONE™ Manuscripts

For Review

Mach Number Effects on Buffeting Flow on a Half Wing-Body Configuration

Abstract

Purpose – A numerical study of the flow over a wing representative of a large civil aircraft at cruise conditions is discussed. For each Mach number, numerical simulations indicate that a critical angle of attack exists where the separated region increases in size and begins to oscillate. This phenomenon, known as transonic shock buffet, is reproduced by the unsteady simulations and much information can be extracted analysing location, amplitude and frequency content of the unsteadiness.

Design/methodology/approach – Reynolds-averaged Navier-Stokes simulations are conducted on a half wing-body configuration, at different Mach numbers and angles of attack. Both steady-state and time-accurate computations are performed. Results are discussed in terms of flow topology and statistical analysis of time-varying quantities.

Findings – The high number of cases presented in this study allows the creation of a database which, to the authors' knowledge, has not been documented in literature before. The results indicate that the unsteady Reynolds-averaged Navier-Stokes approach is capable of describing the main features of the buffet phenomenon.

Research limitations – The presence of a turbulence model, despite allowing the description of the main unsteady phenomenon, might be insufficient to fully characterise the unsteadiness present in transonic flow over a wing. Therefore, researchers are encouraged to confirm, by means of experimental investigation or scale-resolving simulations, the validity of the results obtained from the Reynolds-averaged Navier-Stokes equations.

Practical implications – The results clearly indicate that, despite what has been proposed in recent publications, transonic buffet can be described by means of time-accurate Reynolds-averaged Navier-Stokes equations. Such an approach is popular in the aeronautical industry because of its lower cost compared to higher-fidelity approaches, and could be used for wing design.

Originality/value – The phenomenon of transonic shock buffet on a three-dimensional configuration, important to modern aircraft design, is analysed in great detail. The large number of results presented can be used as a database for future numerical simulations and experiments, and allows the description of the flow physics of the buffet unsteadiness on a half wing-body configuration.

Keywords – Buffet, transonic, unsteady RANS, wing-body configuration.

Type – Research paper.

For Peer Review

1 Introduction

At cruise condition, the flow around a typical civil aircraft is characterised by the presence of shock waves interacting with the boundary layers developing over the wings (Dolling 2001). For combinations of Mach number and angle of attack, a strong interaction can cause the occurrence of large scale unsteadiness such as high-amplitude, self-sustained shock motions, known as shock buffet (Lee 2001). This phenomenon has a significant influence on the aircraft performance and has thus been the subject of numerous studies in the past (Délery & Marvin 1986).

Shock buffet can be observed both in two- and three-dimensional configurations, from simple aerofoils to swept wings. In the two-dimensional case, the unsteadiness is characterised by self-sustained harmonic shock motions. It has been documented by means of experimental (Jacquin et al. 2009, Lee 1990, McDevitt et al. 1976, McDevitt & Okuno 1985, Sugioka et al. 2015) and numerical (Barakos & Drikakis 2000, Brunet 2003, Goncalves & Houdeville 2004, Iovnovich & Raveh 2012, Thiery & Coustols 2006) investigations. Recently, high-fidelity approaches, such as zonal detached-eddy simulation (Deck 2005), have thoroughly described the physics of the flow. From a more fundamental point of view, stability analysis has shown a link between the appearance of shock unsteadiness and the presence of an unstable global mode (Crouch et al. 2009, Iorio et al. 2014, Sartor, Mettot & Sipp 2015).

When considering more complex configurations, such as a wing representative of a large civil aircraft, the unsteady behaviour presents some differences compared to the two-dimensional case (Benoit & Legrain 1987). The literature is more limited and does not agree on the type of shock motions. It has been shown that the frequency spectrum has a distinct peak, especially when considering wings with small sweep angle (Iovnovich & Raveh 2015, Farhangnia et al. 1996). On the contrary, other studies indicate broadband shock movements (Brunet & Deck 2008, Reneaux et al. 2005). In wind-tunnel tests, where the aeroelastic behaviour of the model must be taken into account (Steimle et al. 2012), some authors have reported very broadband pressure spectra in the vicinity of the separated zone (Molton et al. 2013, Dandois 2016), while others have documented narrow peaks in the spectrum of shock location (Caruana et al. 2005). A recent study based on the analysis of two different wind tunnel test campaigns clearly highlighted that on a three-dimensional wing the buffet phenomenon is characterised by a bump in the spectrum which is at a much higher Strouhal number than in 2D (Dandois 2016). Moreover, the work indicated how the buffet phenomenon coexists with the Kelvin-Helmholtz instability developing in the shear layer downstream of the shock foot. This result has also been observed in two-dimensional interactions using global stability analysis (Sartor, Mettot & Sipp 2015, Sartor, Mettot, Bur & Sipp 2015).

In the last decade, several numerical studies have tried to describe the complex shock motions that characterise three-dimensional buffet on a complete wing. Reynolds-averaged Navier-Stokes (RANS) approaches argued that the buffet onset can either be predicted by the presence of massive boundary layer separation (Pearcey 1958) or by the pressure divergence at the trailing edge (Rumsey et al. 2001). Limited results have been produced by unsteady Reynolds-averaged Navier-Stokes (URANS) simulations (Rumsey et al. 2003), and some authors have claimed that a URANS approach is not adapted to reproduce this phenomenon at all (Brunet & Deck 2008). However, shock motions occur at much longer time scales than those of the wall-bounded turbulence, so that URANS simulations can be justified. In this respect, recent studies have presented the capability to simulate transonic tail buffet (Illi et al. 2013) and the shock motions on simple three-dimensional configurations (Iovnovich & Raveh 2015).

The aim of the present paper is thus to describe the transonic flow on a half wing-body configuration by means of RANS and URANS simulations. The work focuses on the characterisation of

For Peer Review

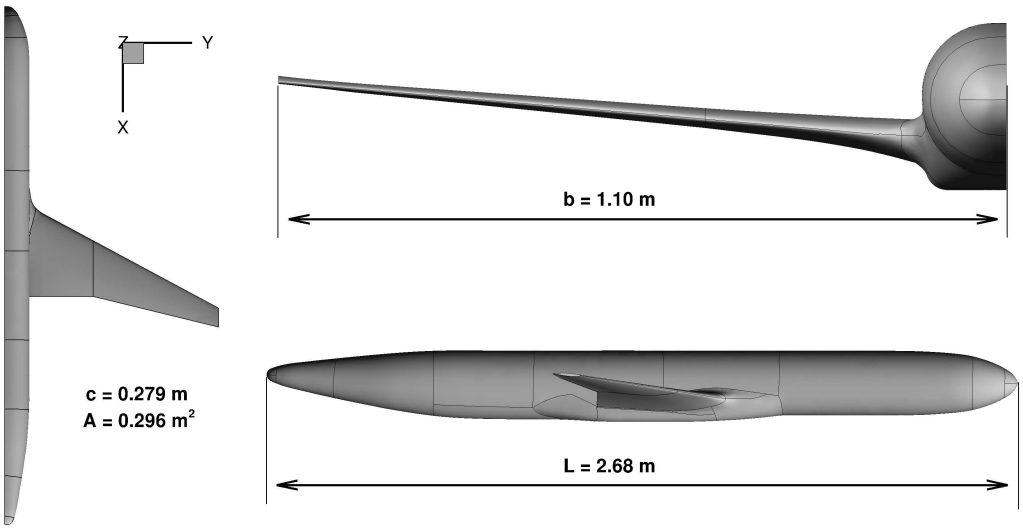

Figure 1: Half wing-body configuration.

For Peer Review

buffet unsteadiness and its onset. It is shown how time-accurate simulations can be used to gain information about the shock motions and their behaviour when considering flows at different Mach numbers. In Section 2 we continue with a description of the test case and the numerical setup, while Section 3 discusses the results of the numerical investigation.

2 Numerical Approach

The half wing-body configuration, chosen as test case, is shown in Figure 1. The wing is twisted, tapered and has a constant sweep angle of 25 deg. The flow conditions are imposed to reproduce the aerodynamic conditions of related wind tunnel tests (Lawson et al. 2016), not discussed in this article. The reference temperature and pressure are 266.5 K and 66.0 kPa, respectively. Six Mach numbers between 0.74 and 0.84 are considered, and the Reynolds number, based on the aerodynamic mean chord, is 3.75 million. Laminar to turbulent transition is imposed on the lower surface at about 5% of local chord, while on the upper surface this is at about 10% outboard of the crank and at 15% inboard.

The simulations are performed using the unstructured finite volume solver DLR-TAU. The second order central scheme with scalar artificial dissipation is used for the convective fluxes of the mean flow equations, while a first order Roe scheme is applied to those of the turbulence model. Convergence is achieved using local time stepping and an implicit Backward Euler solver with Lower-Upper Symmetric Gauss-Seidel iterations. Second order time-accurate computations additionally use the standard dual-time stepping approach. A previous study focussing on a single Mach number was carried out to investigate the turbulence-model dependency (Sartor & Timme 2015). In the present work, two of those turbulence models are considered including the negative Spalart-Allmaras (SA) model (Allmaras et al. 2012) and an explicit algebraic Reynolds-stress model in the form of Realizable Quadratic Eddy Viscosity Model (RQEVM) (Rung et al. 1999).

Using the RANS approach, the imposed angle of attack is increased from zero until the buffet phenomenon is fully developed and about 24 configurations are considered per turbulence model and Mach number. Results of the RANS equations are then used as a starting point for unsteady

computations. The time discretisation is switched to dual-time stepping and every time step is iterated until a convergence criterion, defined below, is reached. The total physical time simulated is 0.09 s for each case, corresponding to approximately 30 buffet cycles. A transient part can be observed in the simulations, where the unsteadiness is built up. Once this transient has passed, time histories of force and moment coefficients, as well as the mean and standard deviation of all flow variables are recorded. A total of 50 and 40 cases have been time-accurately simulated for SA and RQEVM, respectively, using roughly 48 cores of Intel Xeon X5660 processors.

For an unsteady simulation, a time-step size has to be chosen depending on the time scale of the flow unsteadiness. A convergence study has previously been carried out for a Mach number of 0.8, concluding that the time step size should be smaller than 5 μs (Sartor & Timme 2015). Since temporal convergence has been investigated for one particular configuration, a lower time-step size of 2 μs has been chosen for all URANS simulations. This precaution has been taken to prevent inaccuracy in case the buffet frequency is significantly higher for some combination of angle of attack and free-stream Mach number. This value is almost three orders of magnitude smaller than the convective time, defined by the aerodynamic mean chord and reference velocity, which for this case is around 10^{-3} s. Finally, it has to be considered that the shock-induced separation changes in size during a buffet cycle, depending on the shock position. Instead of performing a fixed number of iterations per time step, a Cauchy convergence criterion is applied with the drag coefficient as control variable. Hence, each time step is iterated until a relative error of less than 10^{-8} is found in the previous 20 inner iterations. This criterion results in more iterations when in presence of a massive separation and fewer when the flow is fairly smooth and thus easily converged.

A family of three unstructured meshes produced using the Solar grid generator (Martineau et al. 2006) has been investigated previously focussing on Mach number 0.8 (Sartor & Timme 2015). After the grid dependency has been assessed, only the coarse mesh is retained for the present study. The first cell spacing normal to the viscous walls is less than $y^+ = 0.8$ for all flow conditions, while the growth rate of cell sizes in the viscous layer is less than 1.3. On the wing surface, the characteristic space direction is 0.5% of the span in the root region, while close to the wing tip is around 0.1%. On each wing section, the blunt trailing edge, which plays a central role in the buffet onset (Rumsey et al. 2001), is described by 8 cells with a local spacing of about 0.15% of the local chord.

3 Results

First, steady-state results are analysed. Figure 2 presents the drag polars for four of the considered Mach numbers. The results of the steady RANS approach using local time stepping are shown as solid lines, while the dash-dotted lines are the time-averaged solution of unsteady simulations. It can be seen that the predicted values of lift and drag coefficients are in reasonable agreement comparing the two turbulence models. When the incidence is small, the RANS simulations converge towards a steady-state solution (squared symbols in the figures). After a threshold depending on Mach number, angle of attack and turbulence model, the steady solutions fail to converge, and a time-accurate simulation is needed.

For both turbulence models and smaller Mach numbers, an abrupt change in the polar line occurs when the simulations fail to converge. This distinct slope change (or kink), also observed in other studies, is often used as an indicator of the presence of unsteadiness. In this respect, Pearcey & Holder (1962) showed experimentally that this kink in the lift curve often coincides with buffet onset as measured with a strain gauge on a two-dimensional aerofoil. Focussing on higher Mach

For Peer Review

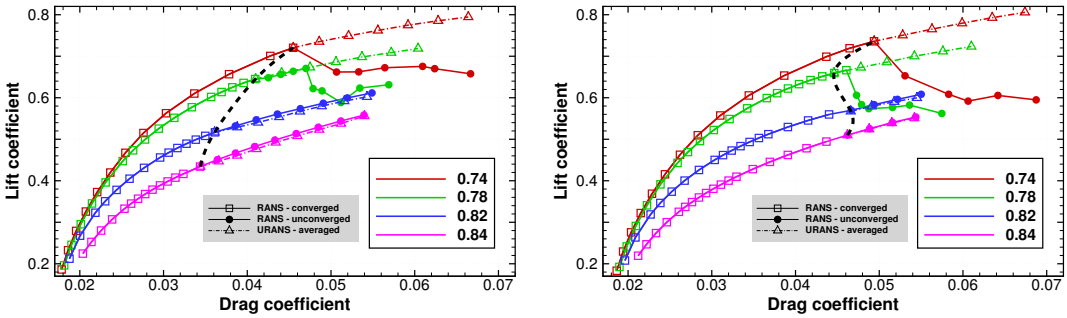

(a) SA turbulence model (b) RQEVM

Figure 2: Drag polars with different turbulence models. Each line represents a Mach number. The black dash-dotted line is the onset condition.

numbers on the other hand, the kink is not observed. In addition, considering the time-averaged results issued from the unsteady simulations, as discussed in more detail below, the drag polars are smooth regardless the presence of unsteadiness.

Although many studies in two-dimensional configurations do not show a clear link between shock buffet and the topology of the flow separation (Crouch et al. 2009, Sartor, Mettot & Sipp 2015), the instability onset is often determined when the separated zone reaches the trailing edge and bursts (Pearcey 1958, Thomas & Redeker 1971). Thus, another common method to predict the presence of unsteadiness and its position is to analyse the distribution of the sectional lift coefficient along the wing span. For this purpose, the pressure coefficient of each steady-state solution is extracted along several wing sections and the contribution of each section to the total lift is calculated.

The results are presented in Figure 3 for the SA turbulence model, showing the sectional lift from wing root to wing tip. The presence of the crank can be noticed by a small discontinuity at 42% of the span. Since the wing is twisted, the positive washout is responsible for the decreasing lift while approaching the wing tip. For each Mach number, inboard of the crank and in its vicinity, the sectional lift coefficients keep increasing constantly with the angle of attack. Outboard of the crank, the pressure loss due to the shock-induced separation causes an abrupt drop in the local lift. A further increase in the angle of attack is responsible for a wider decrease, indicating that the recirculation zone moves towards the fuselage.

By comparing the different plots in Figure 3, it can also be noticed that the pressure drop due to the shock-induced separation is more distinct for lower Mach numbers, indicating a stronger interaction. This could be a consequence of the fact that the separation occurs for higher angle of attack, causing a thicker separated zone. On the contrary, for the Mach number 0.84 shown in Figure 3f the lift coefficient in sections around 75% span remains between 0.42 and 0.46 for all angles of attack greater than 1.6 deg. This indicates that the separated zone is not moving in the spanwise direction, but only increasing its chord-wise extent. In this respect, the lift drop in the figure grows stronger while increasing the angle of attack.

Although not explicitly shown, similar results are obtained with RQEVM in terms of local lift distribution and pressure drop when increasing the Mach number. Consistently with the observations made when discussing steady-state simulations, higher angles of attack are needed to predict the presence of large separation. The results confirm that a link can be found between the abrupt sectional lift decrease and the appearance of unsteadiness. However, one should keep in mind that for those angles of attack the RANS simulation does not converge, indicating the

For Peer Review

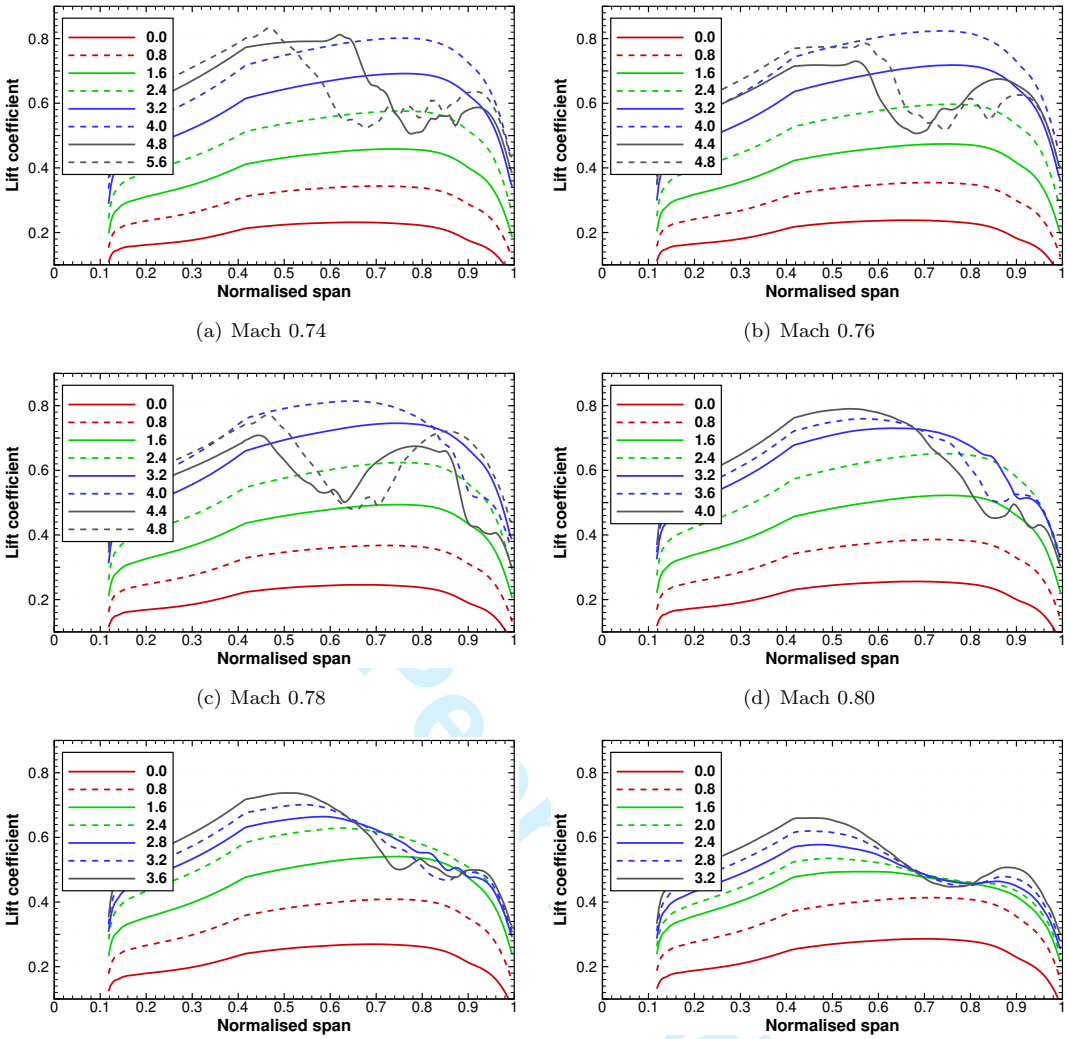

(a) Mach 0.74 (b) Mach 0.76

(c) Mach 0.78 (d) Mach 0.80

(e) Mach 0.82 (f) Mach 0.84

Figure 3: Span-wise distribution of sectional lift coefficient for SA turbulence model. Each colour and line style represents a different angle of attack.

requirement of an unsteady approach.

Time-accurate results are discussed next. Figure 4 presents the time evolution of the lift coefficient and its corresponding power spectral density (PSD). From the time histories, presented in the left column of the figure, it can be seen that up to 0.02 s are needed for the flow to establish the fully developed shock buffet regime. When the Mach number is high, the lift coefficient does not significantly diverge from its steady-state value. Focussing on Mach numbers 0.74 to 0.78 on the other hand, the time-average of the unsteady simulation is not close to the flow field predicted by the steady approach. Comparing with Figure 2, it can be concluded that a sudden change in the aerodynamic loads (or a kink in the drag polars) is not an indicator of the presence of unsteady flow, as suggested by Gariépy et al. (2013), but only a consequence of RANS simulations not converging towards a steady state close to the time-average of the unsteady flow.

The solid lines in Figure 4 have been obtained using the SA turbulence model, while the dash-dotted lines refer to the RQEVM. For all cases, a satisfying agreement is observed when comparing

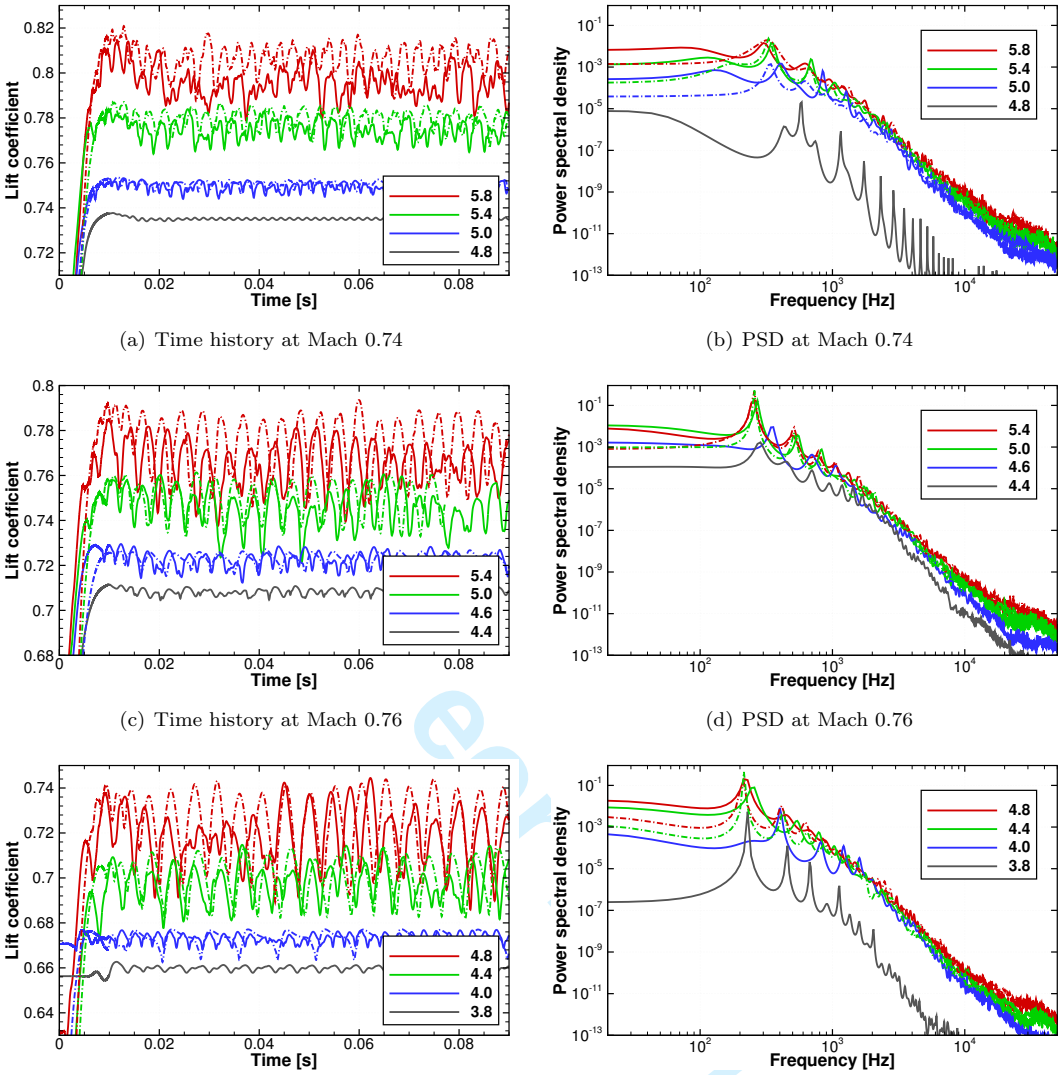

(a) Time history at Mach 0.74

(b) PSD at Mach 0.74

(c) Time history at Mach 0.76

(d) PSD at Mach 0.76

(e) Time history at Mach 0.78

(f) PSD at Mach 0.78

Figure 4: Time history and power spectral density of lift coefficients for SA turbulence model (solid line) and RQEVM (dash-dotted line). Each colour represents a different angle of attack.

average value and amplitude of the fluctuations. The main difference between the two models is the onset. Not only is the critical value of the angle of attack smaller for the SA model, but close to the onset this model also predicts fluctuations which have a simple frequency content. Similar behaviour is not observed for RQEVM. This feature will be discussed in more detail when analysing the frequency content of the signals. By comparing results for increasing Mach number, it can be seen that the onset is shifted to smaller angles of attack, as observed in two-dimensional flows by McDevitt & Okuno (1985). Then, when unsteadiness occurs, the average value of the lift is smaller (note that the vertical axis is adjusted in each plot), and also the amplitude of the fluctuations is more limited (the scale does not change in the plots).

As pointed out previously (Deck & Nguyen 2004), numerical signals issued from CFD are often oversampled and have a short duration. To overcome the problem of the limited spectrum definition we used an autoregressive estimator (Kay & Marple 1981), rather than a traditional Fast

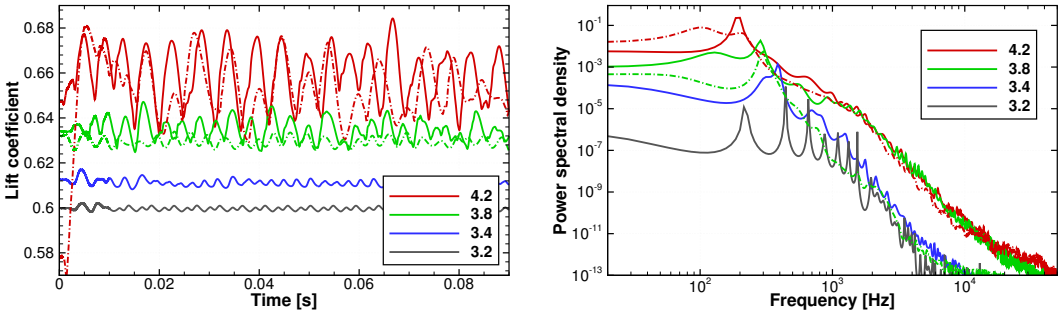

(g) Time history at Mach 0.80 (h) PSD at Mach 0.80

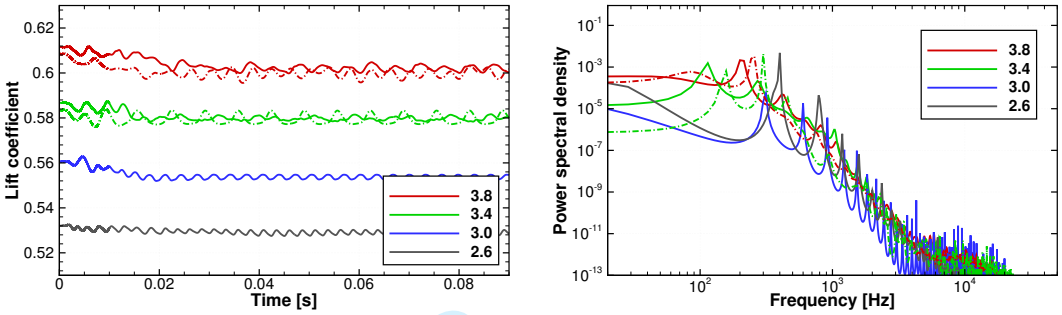

(i) Time history at Mach 0.82 (j) PSD at Mach 0.82

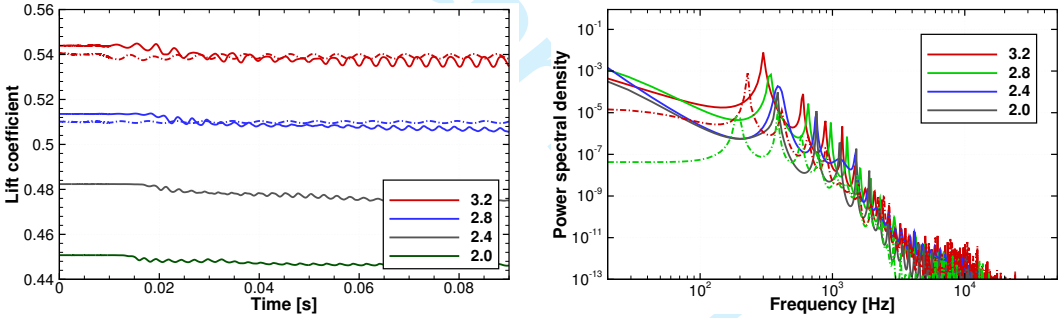

(k) Time history at Mach 0.84 (l) PSD at Mach 0.84

Figure 4: (continued) Time history and PSD of lift coefficients for SA turbulence model (solid line) and RQEVM (dash-dotted line). Each colour represents a different angle of attack.

Fourier Transform. Following the steps of Deck (2005), the power spectral density is computed using Burg's method (Burg 1978). Each case is analysed using a single window covering the total duration of the lift signal without the initial transient. The results are presented on the right column of Figure 4.

In all plots the power spectral density seems to be characterised by a narrowband frequency content for small angles of attack. At onset condition, the signals are not only periodic, but also characterised by a single-frequency harmonic motion. For example, at Mach 0.78 (Figure 4f) the onset condition occurs at narrowband frequency, with a distinguish peak centred at 220 Hz. The presence of these periodic motions can be noticed also in Figure 4e. When increasing the angle of attack, the lift signal presents greater shock motions and, as a consequence, the power spectral density peak is more energetic. A further increase in the angle of attack is responsible for this peak to move towards lower frequency and to become wider. The shock unsteadiness is now

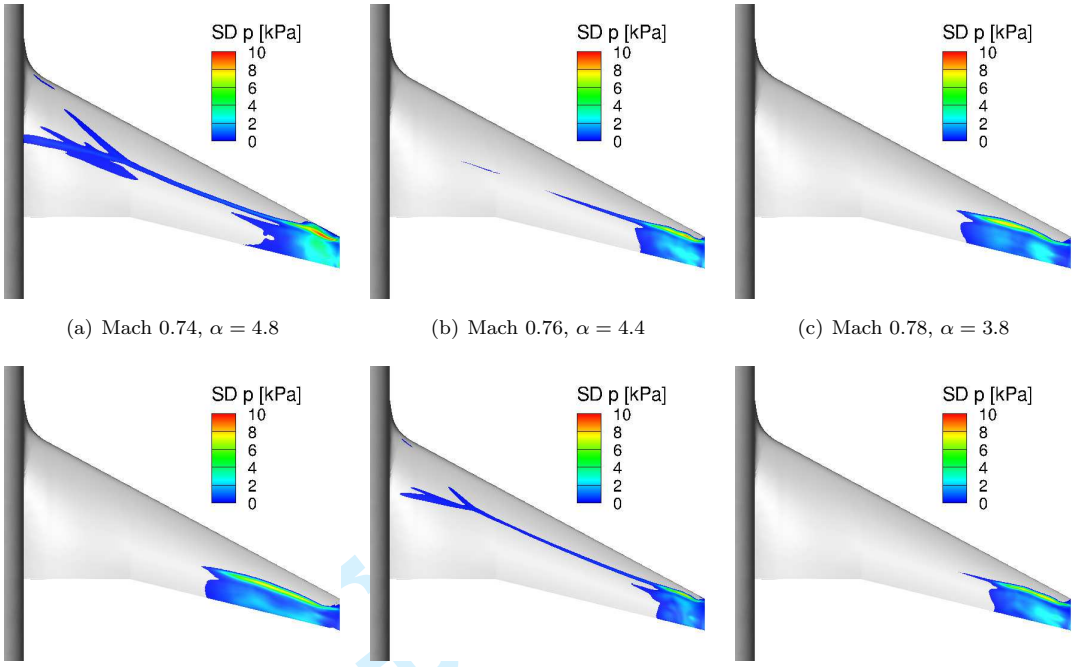

(a) Mach 0.74, $\alpha = 4.8$ (b) Mach 0.76, $\alpha = 4.4$ (c) Mach 0.78, $\alpha = 3.8$

(d) Mach 0.80, $\alpha = 3.2$ (e) Mach 0.82, $\alpha = 2.6$ (f) Mach 0.84, $\alpha = 2.0$

Figure 5: Standard deviation (SD) of pressure at onset conditions.

characterised by non-periodic motions. This behaviour is visible in all plots of Figure 4. When focussing on the highest Mach numbers, the peaks are generally more narrow, which is consistent with the observations in the time-histories of the lift coefficient. In addition, the energy contained in the unsteadiness is lower for those cases.

Focussing on RQEVM, a similar behaviour is observed comparing cases at the same flow conditions. The onset occurs at a higher angle of attack and with a frequency content characterised by broadband unsteadiness from the beginning. Overall, shock motions occur around 100 to 400 Hz. This corresponds, when scaled by a non-dimensional frequency given by the inverse of the convective time, to a Strouhal number of about 0.1 to 0.4. Similar values have been found from experimental investigation (Sugioka et al. 2015) on the Nasa Common Research Model at similar flow conditions and simulation by means of detached-eddy simulation Brunet & Deck (2008).

During the unsteady simulations the variance of the fluctuating pressure is computed. This quantity gives access to the spatial distribution of the unsteady part of the flow. Figures 5 and 6 present the pressure standard deviation, evaluated on the wing surface, at onset conditions and when the buffet is developed, respectively, for the SA turbulence model only. When the angles of attack are small, the shock trace lays on a straight line between the leading and trailing edge. The unsteady separated zone is only in the wing-tip region. For all Mach numbers, the unsteady zones grows bigger with increasing angle of attack, and the centre of the unsteadiness moves towards the fuselage, in agreement with Sugioka et al. (2015). In addition, the shock trace bends (Figure 6c) or even adopts a serpentine shape (Figure 6f).

Comparing all cases, it can be noticed that the separated zone is more limited when the Mach number is small, while the whole shock foot is unsteady. This occurs regardless the presence of separation, also inboard of the crank and already from onset. For some cases the shock foot is unsteady even on the fuselage (Figure 6a-b). On the contrary when focussing on cases with

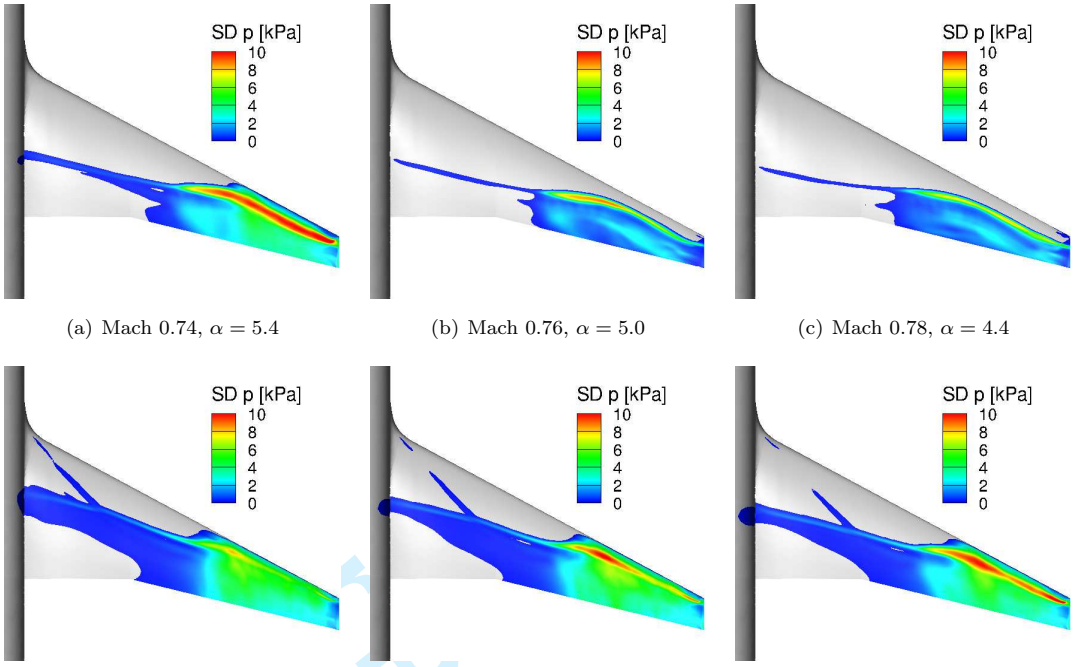

(a) Mach 0.74, $\alpha = 5.4$ (b) Mach 0.76, $\alpha = 5.0$ (c) Mach 0.78, $\alpha = 4.4$

(d) Mach 0.80, $\alpha = 3.8$ (e) Mach 0.82, $\alpha = 3.4$ (f) Mach 0.84, $\alpha = 2.8$

Figure 6: Standard deviation (SD) of pressure when buffet unsteadiness is fully developed.

the highest Mach number, no unsteady flow can be found on the leading edge, even when the unsteadiness is fully developed (Figure 6e-f). Overall, very similar shock-foot traces have been observed in numerical studies on a tapered and swept wing (Brunet & Deck 2008), non-tapered swept configuration (Iovnovich & Raveh 2015), and experiments (Sugioka et al. 2015).

Figure 7 summarises the major results in terms of unsteadiness for all Mach numbers and angles of attack. Each symbol has been obtained by computing the standard deviation of the lift coefficient in a time-accurate simulation, once the transient has passed. A zero standard deviation indicates the absence of unsteadiness in the flow, while high values describe large shock motions. The unsteady content is more distinct for low Mach numbers, and the magnitude of unsteadiness keeps increasing with the angle of attack. For higher Mach numbers, the magnitude of unsteadiness reaches a plateau, and increasing the angle of attack does not seem to affect the magnitude of the shock motions.

Comparing Figures 7a and 7b it can be seen that there is a good agreement between the two turbulence models when the Mach number is small. When focussing on higher Mach numbers, the RQEVM predicts an onset of the unsteadiness for greater angles of attack. The difference in the onset angle goes up to 0.8 deg for Mach 0.84. Then, once the unsteadiness is fully developed, similar values of the standard deviation are observed.

4 Conclusions

The flow over a typical large civil aircraft at cruise conditions has been analysed using a half wing-body model and Reynolds-averaged Navier-Stokes modelling. Steady-state solutions converge only when the flow does not present a large separated zone on the upper surface of the wing. Time-accurate simulations have then to be considered. For low angles of attack, the shock-induced

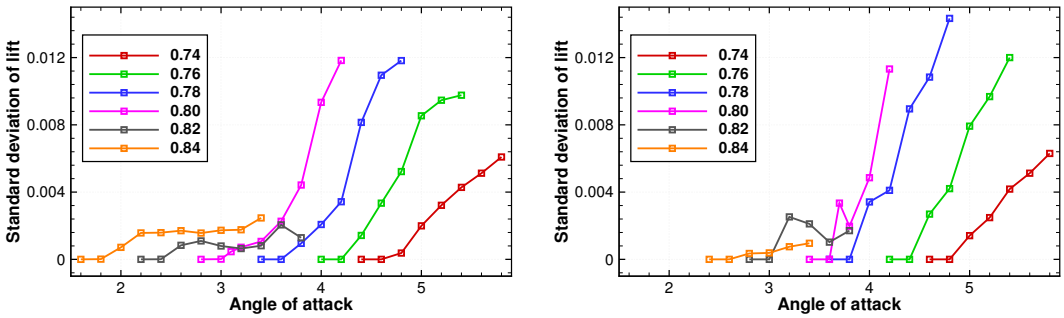

(a) SA turbulence model (b) RQEVM

Figure 7: Standard deviation of lift coefficient vs angle of attack. Each colour represents a different Mach number, each point is obtained with a different URANS simulation.

separation has a limited size and the flow is steady. Increasing the angle of attack, the separated zone begins to oscillate, starting close to the wing tip and then moving inboard. An increasingly broadband frequency content can be observed, while the most energetic frequency in the power spectral density decreases.

Comparing the buffet phenomenon at different Mach numbers, the onset of the unsteadiness occurs for smaller angles of attack when increasing the Mach number. Similar frequency content is then observed for different cases. Focussing on the magnitude of the unsteadiness, the standard deviation of the lift coefficient is lower for high Mach numbers, and reaches a plateau immediately after the onset. In these cases, only the separated zone is unsteady. For lower Mach numbers, although the separated zone has a reduced size, the unsteadiness can be observed on the entire wing. The amplitude of the shock motions increases constantly when increasing the angle of attack.

The high number of cases presented in this study allows the creation of a database which, to the authors' knowledge, has not been documented in literature before. Previous studies were able to compare flow conditions at different angles of attack only for two-dimensional cases. More realistic studies on half-wing body configurations were limited to few angles of attack and one Mach number. The results presented indicate that an unsteady Reynolds-averaged Navier-Stokes approach is capable of describing the main features of the buffet phenomenon.

Acknowledgments

The research leading to these results has received funding from the European Union's Seventh Framework Programme (FP7/2007-2013) for the Clean Sky Joint Technology Initiative under grant agreement n° 336948.

References

Allmaras, S. R., Johnson, F. T. & Spalart, P. R. (2012), Modifications and clarifications for the implementation of the Spalart-Allmaras turbulence model, *in* 'ICCFD7-1902, 7th International Conference on Computational Fluid Dynamics, Big Island, Hawaii'.

Barakos, G. & Drikakis, D. (2000), 'Numerical simulation of transonic buffet flows using various turbulence closures', *International Journal of Heat and Fluid Flow* **21**(5), 620–626.

http://mc.manuscriptcentral.com/hff

For Peer Review

Benoit, B. & Legrain, I. (1987), 'Buffeting prediction for transport aircraft applications based on unsteady pressure measurements', *AIAA Paper 87–2356* .

Brunet, V. (2003), 'Computational study of buffet phenomenon with URANS equations', *AIAA Paper 2003–3679* .

Brunet, V. & Deck, S. (2008), Zonal-detached eddy simulation of transonic buffet on a civil aircraft type configuration, *in* 'Advances in Hybrid RANS-LES Modelling', Springer, pp. 182–191.

Burg, J. P. (1978), Maximum entropy spectral analysis, *in* 'Modern Spectrum Analysis', Edited by D. G. Childers, IEEE Press, New York, pp. 34–41.

Caruana, D., Mignosi, A., Corrègeand, M., Pourhiet, A. L. & Rodde, A. M. (2005), 'Buffet and buffeting control in transonic flow', *Aerospace science and technology* **9**(7), 605–616.

Crouch, J. D., Garbaruk, A., Magidov, D. & Travin, A. (2009), 'Origin of transonic buffet on aerofoils', *Journal of Fluid Mechanics* **628**, 357–369.

Dandois, J. (2016), 'Experimental study of transonic buffet phenomenon on a 3d swept wing', *Physics of Fluids* **28**(1), 016101.

Deck, S. (2005), 'Numerical simulation of transonic buffet over the OAT15A airfoil', *AIAA Journal* **43**(7), 1556–1566.

Deck, S. & Nguyen, A. T. (2004), 'Unsteady side loads in a thrust-optimized contour nozzle at hysteresis regime', *AIAA Journal* **42**(9), 1878–1888.

Délery, J. & Marvin, J. G. (1986), 'Shock-wave boundary layer interactions', *AGARDograph No. 280* .

Dolling, D. S. (2001), 'Fifty years of shock-wave/boundary-layer interaction research: what next?', *AIAA Journal* **39**(8), 1517–1531.

Farhangnia, M., Guruswamy, G. P. & Biringen, S. (1996), 'Transonic-buffet associated aeroelasticity of a supercritical wing', *AIAA Paper 96–0286* .

Gariépy, M., Malouin, B., Trépanier, J.-Y. & Laurendeau, É. (2013), 'Far-field drag decomposition applied to the drag prediction workshop 5 cases', *Journal of Aircraft* **50**(6), 1822–1831.

Goncalves, E. & Houdeville, R. (2004), 'Turbulence model and numerical scheme assessment for buffet computations', *International journal for numerical methods in fluids* **46**(11), 1127–1152.

Illi, S. A., Fingskes, C., Lutz, T. & Krämer, E. (2013), 'Transonic tail buffet simulations for the common research model', *AIAA Paper 2013–2510* .

Iorio, M. C., González, L. M. & Ferrer, E. (2014), 'Direct and adjoint global stability analysis of turbulent transonic flows over a naca0012 profile', *International Journal for Numerical Methods in Fluids* **76**(3), 147–168.

Iovnovich, M. & Raveh, D. E. (2012), 'Reynolds-Averaged Navier-Stokes study of the shock-buffet instability mechanism', *AIAA Journal* **50**(4), 880–890.

Iovnovich, M. & Raveh, D. E. (2015), 'Numerical study of shock buffet on three-dimensional wings', *AIAA Journal* **53**(2), 449–463.

For Peer Review

Jacquin, L., Molton, P., Deck, S., Maury, B. & Soulevant, D. (2009), 'Experimental study of shock oscillation over a transonic supercritical profile', *AIAA Journal* **47**(9), 1985–1994.

Kay, S. M. & Marple, S. L. J. (1981), 'Spectrum analysis – a modern perspective', *Proceedings of the IEEE* **69**(11), 1380–1419.

Lawson, S. G., Greenwell, D. & Quinn, M. (2016), 'Characterisation of buffet on a civil aircraft wing', *AIAA Paper 2016–1309* .

Lee, B. H. K. (1990), 'Oscillatory shock motion caused by transonic shock boundary-layer interaction', *AIAA Journal* **28**(5), 942–944.

Lee, B. H. K. (2001), 'Self-sustained shock oscillations on airfoils at transonic speeds', *Progress in Aerospace Sciences* **37**(2), 147–196.

Martineau, D. G., Stokes, S., Munday, S. J., Jackson, A. P., Gribben, B. J. & Verhoeven, N. (2006), 'Anisotropic hybrid mesh generation for industrial rans applications', *AIAA Paper 2006-534* .

McDevitt, J. B., Levy, J. L. L. & Deiwert, G. S. (1976), 'Transonic flow about a thick circular-arc airfoil', *AIAA Journal* **14**(5), 606–613.

McDevitt, J. B. & Okuno, A. F. (1985), 'Static and dynamic pressure measurements on a NACA 0012 airfoil in the ames high reynolds number facility', *NASA TP-2485* .

Molton, P., Dandois, J., Lepage, A., Brunet, V. & Bur, R. (2013), 'Control of buffet phenomenon on a transonic swept wing', *AIAA Journal* **51**(4), 761–772.

Pearcey, H. H. (1958), A method for the prediction of the onset of buffeting and other separation effects from wind tunnel tests on rigid models, Technical report, DTIC Document.

Pearcey, H. H. & Holder, D. W. (1962), 'Simple methods for the prediction of wing buffeting resulting from bubble type separation', *Aero Rep. 1024* .

Reneaux, J., Brunet, V., Caruana, D., Deck, S. & Naudin, P. (2005), 'A combined experimental and numerical investigation of the buffet phenomenon and its control through passive and active devices.', *ONERA Tiré à Part* **2005**(103).

Rumsey, C. L., Allison, D. O., Biedron, R. T., Buning, P. G., Gainer, T. G., Morrison, J. H., Rivers, S. M., Mysko, S. J. & Witkowski, D. P. (2001), 'Cfd sensitivity analysis of a modern civil transport near buffet-onset conditions', *NASA TM-2001-211263* .

Rumsey, C. L., Morrison, J. H. & Biedron, R. T. (2003), 'Cfd variability for a civil transport aircraft near buffet-onset conditions', *NASA TM-2003-212149* .

Rung, T., Lübcke, H., Franke, M., Xue, L., Thiele, F. & Fu, S. (1999), 'Assessment of explicit algebraic stress models in transonic flows', *Engineering turbulence modelling and experiments 4* pp. 659–668.

Sartor, F., Mettot, C., Bur, R. & Sipp, D. (2015), 'Unsteadiness in transonic shock-wave/boundary-layer interactions: experimental investigation and global stability analysis', *Journal of Fluid Mechanics* **781**, 550–577.

Sartor, F., Mettot, C. & Sipp, D. (2015), 'Stability, receptivity and sensitivity analyses of buffeting transonic flow over a profile', *AIAA Journal* **53**(7), 1980–1993.

For Peer Review

Sartor, F. & Timme, S. (2015), 'Reynolds-Averaged Navier-Stokes simulations of shock buffet on half wing-body configuration', *AIAA Paper 2015–1939. Submitted to AIAA Journal* .

Steimle, P. C., Karhoff, D.-C. & Schröder, W. (2012), 'Unsteady transonic flow over a transport-type swept wing', *AIAA Journal* **50**(2), 399–415.

Sugioka, Y., Numata, D., Asai, K., Koike, S., Nakakita, K. & Koga, S. (2015), 'Unsteady PSP measurement of transonic buffet on a wing', *AIAA Paper 2015–0025* .

Thiery, M. & Coustols, E. (2006), 'Numerical prediction of shock induced oscillations over a 2D airfoil: Influence of turbulence modelling and test section walls', *International Journal of Heat and Fluid Flow* **27**(4), 661–670.

Thomas, F. & Redeker, G. (1971), *A method for calculating the transonic buffet boundary including the influence of Reynolds number*, DFVLR.

For Peer Review